RAPID COMMUNICATIONS

PHYSICAL REVIEW B VOLUME 48, NUMBER 4 15 JULY 1993-II

Linear and circular polarizations of exciton luminescence in GaAs/$Al_xGa_{1-x}As$ quantum wells

A. Frommer, E. Cohen, and Arza Ron
Solid State Institute, Technion–Israel Institute of Technology, Haifa 32000, Israel

L. N. Pfeiffer
AT&T Bell Laboratories, Murray Hill, New Jersey 07974

(Received 7 April 1993)

The cw, linearly and circularly polarized photoluminescence excitation spectra (P_{lin} and P_{cir}), are studied for ($e1$:hh1) excitons of undoped GaAs/$Al_xGa_{1-x}As$ quantum wells. Monitoring in the high-energy range of the luminescence, pronounced $1S$ and $2S$ polarization-preserving bands are observed. They are shown to be due to LA-phonon-assisted relaxation of delocalized excitons. For the low-energy range $P_{lin} \sim 0$ and a circular polarization reversal is observed, resulting from exciton-exciton scattering.

The degree of polarization P that is observed in the photoluminescence (PL) spectrum of e-h pair recombination has been extensively studied both in bulk semiconductors[1–3] and in quantum-well (QW) structures.[4–10] P is determined by the dynamic processes which the e-h pair undergoes during the states of photoexcitation, energy relaxation, and radiative recombination. In doped semiconductors, the degree of circular polarization P_{cir} is determined by the dynamics of the photoexcited minority carriers. Thus, in n-type QW's, P_{cir} is well explained[11,12] by the hole spin-relaxation processes. When the hole undergoes a scattering process, the probability of spin flip depends on the admixture of valence subbands, which, in turn, depends on the hole in-plane wave vector. In photoexcited undoped QW's, at low temperatures, the elementary excitations are excitons. Then, relaxation processes of both the e and h affect P, and thus, its analysis is more complex than that required for doped QW's. Several recent reports[6–9] examined the temporal dependence of P_{cir} in the spectral range of the ($e1$:hh1)$1S$ exciton PL band. The results were analyzed in terms of the e and h spin-relaxation rates and the e-h exchange interaction.[10] Some observations[7,8] indicate that exciton-exciton interaction is an effective spin-flip mechanism. The degree of linear polarization P_{lin} differs from P_{cir} in that any scattering process which changes either the e or the h state results in a complete loss of the exciton linear polarization.[3] A study[5] of $P_{lin}(t)$ for an undoped QW excited selectively in the ($e1$:hh1) PL band indicated that exciton relaxation processes within this band preserve some degree of linear polarization. This was used as an argument for coherent exciton motion over interface islands with dimensions that are larger than the exciton Bohr radius.

All these studies show that P_{cir} and P_{lin} are sensitive probes of the excitonic states and therefore, it is important to understand the spectral dependence of both P_{cir} and P_{lin}. While short-pulse spectroscopy is necessary to obtain relaxation rates, it is, inherently, a low spectral resolution and high exciton density method. On the other hand, cw spectroscopy yields very high spectral resolution and low exciton densities. In this work we studied the cw P_{cir} and P_{lin} spectra, monitored at various energies (E_m) within the ($e1$:hh1)$1S$ band of GaAs/$Al_xGa_{1-x}As$ multiple QW's. We consider both P_{lin} and P_{cir} and the comparison between them in order to identify the dynamic processes which *preserve* the exciton polarization. We find that pronounced $1S$ and $2S$ excitonic features are clearly resolved in the polarization spectra and their analysis demonstrates the importance of both the translational and the internal excitonic states in determining the degree of polarization. In addition, we show that whenever exciton-exciton scattering takes place, this process flips the spin of one of the excitons.

Several undoped GaAs/$Al_{0.33}Ga_{0.67}As$ multiple QW's with well width of $d_w = 50$ Å and GaAs/AlAs QW's with $d_w = 70$ Å were studied. They were grown by molecular-beam epitaxy on (001)-oriented GaAs substrates. All have 200-Å barriers and consist of 50 periods. The samples were placed in an immersion-type Dewar, at $T = 1.6$ K. Excitation was done with a cw dye laser (pyridine 2) pumped by an Ar^+ laser. The laser beam was focused down to a spot of about 0.2 mm in diameter, and the maximum power (at the sample surface) did not exceed 3 W/cm^2. The exciting and emitted light beams were directed within 5° of the QW plane normal. The luminescence was dispersed by a double monochromator (having a spectral resolution of 0.1 meV) and the photomultiplier signal was processed with a lock-in amplifier.

The linear polarization spectrum is defined as $P_{lin}(E_m,E_l)=[I_{\parallel}(E_m,E_l)-I_{\perp}(E_m,E_l)]/[I_{\parallel}(E_m,E_l)+I_{\perp}(E_m,E_l)]$, where E_l is the exciting laser energy and $I_{\parallel}$ ($I_{\perp}$) is the PL intensity polarized parallel (perpendicular) to that of the laser. (P_{cir} is similarly defined.) P_{lin} and P_{cir} were measured by using either fixed linear and circular polarizers, or a photoelastic modulator[13] operating at 50 kHz. Both methods yielded similar results, but the signal-to-noise ratio of the latter was about 10 times better. We also note that P_{lin} was found to be independent of the laser polarization direction in the QW plane.

Since all the studied QW's showed similar P_{lin} and P_{cir}, we present here only the data obtained for a $d_w = 50$ Å

multiple QW. Figure 1(a) shows the absorption, PL, and its excitation (PLE) spectra in the energy range of the (e1:hh1) and (e1:lh1) excitons. The absorption and PLE spectra show the inhomogeneously broadened 1S band as well as the excited nS band of the (e1:hh1) exciton.[14] We find that the large inhomogeneous width of the (e1:hh1)1S band is advantageous for our study. It allows us to obtain a series of PLE, $P_{\rm lin}$, and $P_{\rm cir}$ spectra over a wide range of E_m. Figure 2 shows two sets of such spectra monitored at two energies: in the low-energy part of the PL band [Figs. 2(a)–2(c)] and in its high-energy part [Figs. 2(d)–2(f)]. The last two spectra are shown in greater detail in Fig. 3, which also shows the magnitudes of the observed polarizations: $P_{\rm lin} \leq 10\%$ and $P_{\rm cir} \leq 22\%$. All $P_{\rm lin}$ and $P_{\rm cir}$ monitored at E_m higher than the peak of the PL band are similar to those shown in Fig. 3: they consist of two bands that are denoted 1S and 2S and they both vanish for E_l above the 2S band. We note that strong polarization spectra [such as those shown in Figs. 2(e) and 2(f)] are observed even in the high-energy tail of the PL band, where the total emission is weak. For E_m below the PL band peak, $P_{\rm lin}$ gradually vanishes and $P_{\rm cir}$ loses the 1S and 2S band features and becomes similar to spectra reported by others,[4] *but with an opposite sign.*

We now turn to analyze the spectral features of $P_{\rm lin}$ and $P_{\rm cir}$ by examining the dynamics of an exciton that is created at E_l and recombines at E_m. Recent studies of the PL band shape[15] and of the spectral and temporal dependence of PL (Ref. 16) and of $P_{\rm lin}$ (Ref. 5) lead to the following description: The spatial potential fluctuations (that are due to interface roughness) can localize the exciton on various length scales. If the localization area is larger than πa_{nS}^2 [where a_{nS} is the Bohr radius of the (e1:hh1)nS state], then the exciton in-plane motion can be approximated by a well-defined $\mathbf{K}_\parallel$. Such areas (often called "interface islands") still have short-range roughness[17] that determines the (average) localization of all exciton states in a given island. We thus describe the exciton dispersion relations for a given interface island by $E_{1S}(\mathbf{K}_\parallel), E_{2S}(\mathbf{K}_\parallel), \ldots$ surfaces as shown schematically in Fig. 4. Excitons in different interface islands have similar dispersion relations, and they differ only in $E_{1S}(K_\parallel = 0)$, which is determined by the average potential. We shall refer to these loosely localized excitons as "delocalized." Our study[18] of microwave-modulated PL spectra (of the same samples used here) supports this description of delocalized excitons in the upper part of the PL band. Strictly localized states are those due to deep potential fluctuations, and the corresponding exciton energies are in the lowest part of the PL band. Extended exciton states are those with energies higher than the PL band. The spread in the $E_{1S}(K_\parallel = 0)$ of the delocalized and the extended states gives rise to the inhomogeneous broadening of both the absorption and PLE bands (Fig. 1). We indicate the spectral range of these types of states in Fig. 1.

The dynamic processes which affect $P_{\rm lin}$ and $P_{\rm cir}$ occur

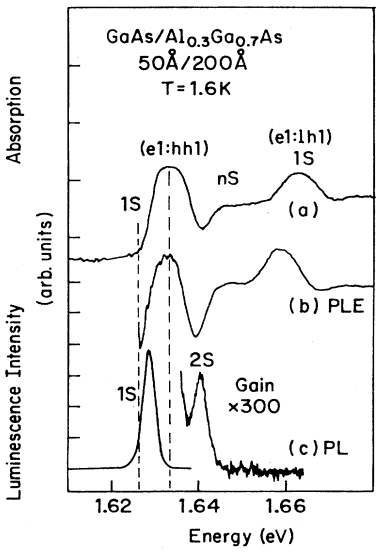

FIG. 1. (a) The absorption spectrum taken with a sample whose substrate was etched away. (b) The photoluminescence excitation spectrum monitored in the lower-energy part of the luminescence band ($E_m = 1.625$ eV). (c) The photoluminescence spectrum excited deep into the conduction band. The two vertical dotted lines are the demarcation between localized (lower-energy tail), delocalized (middle), and extended exciton states.

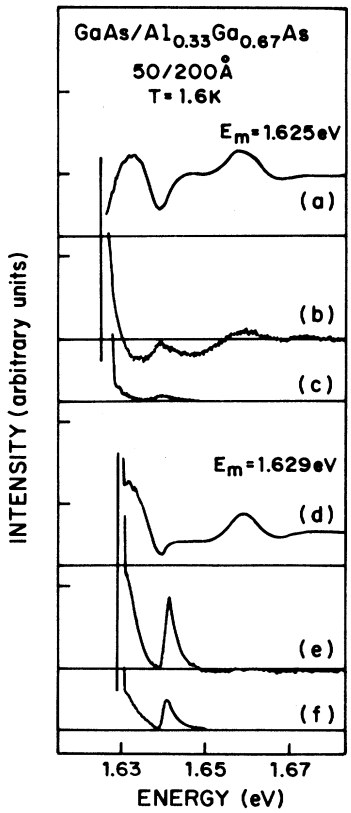

FIG. 2. (a) PLE, (b) $P_{\rm cir}$, (c) $P_{\rm lin}$. All are monitored at the bottom of the PL band, in the range of localized excitons. (d)–(f) are the same as (a)–(c) but monitored in the high-energy part of the PL band, in the range of delocalized excitons. (The vertical solid lines indicate the monitored energy.)

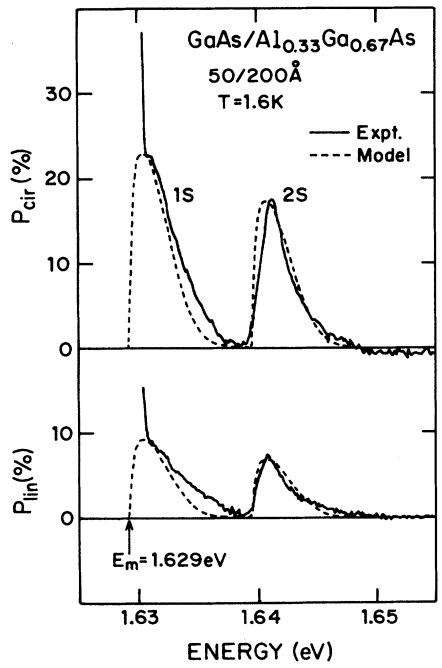

FIG. 3. A detailed spectrum of $P_{\rm lin}$ and $P_{\rm cir}$, monitored in the delocalized exciton region (solid curves). The dashed curves are the calculated rate of inelastic exciton–LA-phonon scattering ($\Gamma_{\rm LA}$). The same calculated function is fitted to each of the bands ($1S$ and $2S$) of $P_{\rm lin}$ and $P_{\rm cir}$.

in the following stages of the exciton life: (a) photoexcitation at energy $E_l = E_{1S}(\mathbf{K}'_{\parallel}=0)$; (b) elastic scattering from the island with E_l into the one where the exciton recombines; (c) relaxation into the recombination state within this island; (d) recombination at $E_{1S}(K_{\parallel}=0)=E_m$. Figure 4 schematically shows the two first stages in cases where the photoexcited exciton scatters elastically (dotted arrows) into either the $1S$ or the $2S$ band of the interface island with E_m. When this E_m is in the range of *delocalized excitons,* the resulting $1S$ and $2S$ bands of the $P_{\rm lin}$ and $P_{\rm cir}$ spectra have sharper features than those of the unpolarized PLE spectrum [cf. Figs. 2(d)–2(f)]. This means that only part of all possible exciton relaxation routes from E_l to E_m contribute to $P_{\rm lin}$ and $P_{\rm cir}$. We take

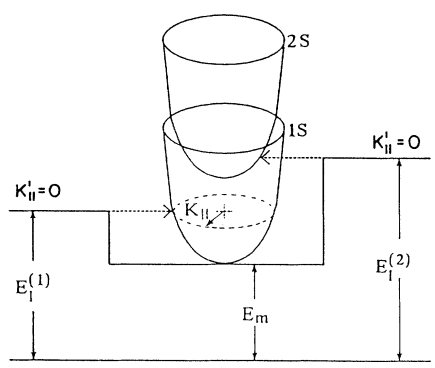

FIG. 4. A schematic description of the model used to interpret the polarization spectra. See text.

these to be the single acoustic-phonon scattering processes which occur within the island where the exciton recombines. For the case of excitation at $E_l^{(1)}$, the exciton is scattered elastically into $E_{1S}(\mathbf{K}_{\parallel})=E_l^{(1)}$, and then inelastically by emitting a phonon with energy $\hbar\omega(\mathbf{Q})=E_{1S}(\mathbf{K}_{\parallel})-E_m(\mathbf{K}_{\parallel}=0)$. Stolz *et al.*[5] have shown that LA phonons interact much more effectively with the exciton than TA phonons. They (and Takagahara[19]) have calculated the exciton–LA-phonon scattering rate, and we use their results in order to calculate the total scattering rate $\Gamma_{\rm LA}(\hbar\omega)$ for excitons in the $1S$ state. Since the LA phonons (with a fixed energy $\hbar\omega$) can have $\mathbf{Q}=(\mathbf{Q}_{\parallel},Q_z)$ and Q_z is unrestricted, we sum over all in-plane phonon wave vectors, subject to the condition $Q_{\parallel}=K_{\parallel}=\hbar^{-1}[2M_X(E_l-E_m)]^{1/2}$. M_X is the translational exciton mass. Using the parameters of Ref. 19, the calculated $\Gamma_{\rm LA}(\hbar\omega)$ is shown in Fig. 3. The same $\Gamma_{\rm LA}$ function is drawn for the $1S$ and $2S$ bands of both $P_{\rm lin}$ and $P_{\rm cir}$, with the following adjustments to the experimental curves: For the $1S$ branches, $\Gamma_{\rm LA}(\hbar\omega=0)$ is set at E_m, and its peak value is adjusted to fit the highest $P_{\rm lin}$ or $P_{\rm cir}$ (disregarding scattered laser light near E_m). For the $2S$ branch, the highest point of $\Gamma_{\rm LA}$ is adjusted to fit the highest value of $P_{\rm lin}$ or $P_{\rm cir}$. Several conclusions can be drawn from the good agreement between the calculated $\Gamma_{\rm LA}$ and the observed polarization spectra. First, for the $1S$ band, $P_{\rm lin}$ and $P_{\rm cir}$ are large whenever $\Gamma_{\rm LA}$ is high. In other words, the faster the exciton relaxes from E_l into E_m, the larger is the polarization preservation. This means that the dynamic processes which lead to randomization of the exciton polarization must occur when the exciton moves (with a given kinetic energy) in the island where it recombines. These processes can be elastic scattering by impurities or short-range interface fluctuations. Second, the same $\Gamma_{\rm LA}$ function fits the $2S$ bands of both $P_{\rm lin}$ and $P_{\rm cir}$. This suggests that when the exciton scatters into the $2S$ branch [i.e., $E_l=E_{2S}(\mathbf{K}_{\parallel})$], its most probable subsequent relaxation (within the island where it recombines) is by a vertical transition into $E_{1S}(\mathbf{K}_{\parallel})$, followed by an emission of an additional LA phonon with $\mathbf{Q}_{\parallel}=\mathbf{K}_{\parallel}$.

Finally we consider the spectral features observed in $P_{\rm lin}$ and $P_{\rm cir}$ for E_m in the range of localized excitons [cf. Figs. 2(a)–2(c)]. For near resonant excitation ($E_l-E_m \leq 3$ meV), the polarization is preserved, namely, $P_{\rm lin}>0$ and $P_{\rm cir}>0$. (This excitation is by acoustic-phonon-assisted optical absorption.) For higher E_l a different behavior is observed: $P_{\rm lin}\sim 0$ and $P_{\rm cir}<0$ in the ($e1$:hh1) range and $P_{\rm cir}>0$ in the ($e1$:lh1) range. [The spectra shown in Figs. 2(b) and 2(c) still show the $2S$ band. For lower E_m, $P_{\rm lin}$ strictly vanishes and the $2S$ band in $P_{\rm cir}$ is unobserved.] The photoexcited excitons at E_l are either delocalized or extended and can be scattered by the localized excitons at E_m. In such a scattering process, either e or h (or both) of the localized exciton change their state, leading to $P_{\rm lin}=0$. The fact that $P_{\rm cir}<0$ in the ($e1$:hh1) range means that the same scattering process preferentially reverses the polarization of the recombining exciton. More specifically, consider excitation (at E_l) with σ^+ polarization which creates a steady

state $|+1\rangle_m$ exciton population at E_m. These excitons are subjected to scattering by a high flux of $|+1\rangle_l$ excitons at E_l. If the transient state (formed during the scattering process) of $|+1\rangle_l|+1\rangle_m$ has a higher total energy than the $|+1\rangle_l|-1\rangle_m$ state, then there will be a preferential polarization reversal of the exciton in the emitting state. Indications that such an exciton-exciton interaction reverses the circular polarization were found in two recent studies of $P_{\rm cir}(t)$.[7,8]

In summary, we have compared the $P_{\rm lin}$ and $P_{\rm cir}$ spectra monitored throughout the $(e1{:}{\rm hh}1)1S$ exciton PL band and excited within the whole excitonic absorption band. The dominant spectral features in these spectra are the $1S$ and $2S$ bands. We interpret these results by assuming that delocalized excitons can be described by a well-defined in-plane wave vector and, consequently, both their $P_{\rm lin}$ and $P_{\rm cir}$ spectra can be well fitted by the exciton–LA-phonon scattering rate function. It means that the exciton depolarizes by elastic scattering processes which occur while it moves over large-scale interface islands. For exciton recombination in the low-energy tail of the PL band, $P_{\rm lin}\sim 0$ and $P_{\rm cir}$ is reversed. We propose that this is due to scattering of delocalized excitons (at E_l) by the localized ones (at E_m). This scattering is preferentially circular-polarization reversing.

The work at Technion was supported by the United States–Israel Binational Science Foundation (BSF), Jerusalem, Israel and was done at the Center for Advanced Opto-Electronics Research.

[1] *Optical Orientation,* edited by F. Meier and B. P. Zakharchenya (North-Holland, Amsterdam, 1985).

[2] G. E. Pikus and E. L. Ivchenko, in *Excitons,* edited by E. I. Rashba and M. D. Sturge (North-Holland, Amsterdam, 1982), p. 205.

[3] R. Planel and C. Benoit à la Guillaume, in *Optical Orientation* (Ref. 1), p. 353.

[4] R. C. Miller and D. A. Kleinman, J. Lumin. **30**, 520 (1985).

[5] H. Stolz, D. Schwarze, W. von der Osten, and G. Weimann, Superlatt. Microstruct. **6**, 271 (1989).

[6] T. C. Damen, K. Leo, J. Shah, and J. E. Cunningham, Appl. Phys. Lett. **58**, 1902 (1991).

[7] T. C. Damen, L. Viña, J. E. Cunningham, and J. Shah, Phys. Rev. Lett. **67**, 3432 (1991).

[8] S. Bar-Ad and I. Bar-Joseph, Phys. Rev. Lett. **68**, 349 (1992).

[9] J. B. Stark, W. H. Knox, and D. S. Chemla, Phys. Rev. Lett. **68**, 3080 (1992).

[10] M. J. Snelling, E. Blackwood, R. T. Harley, P. Dawson, and C. T. B. Foxon (unpublished).

[11] T. Uenoyama and L. J. Sham, Phys. Rev. Lett. **64**, 3070 (1990).

[12] R. Ferreira and G. Bastard, Phys. Rev. B **43**, 9687 (1991).

[13] K. W. Hipps and G. A. Crosby, J. Phys. Chem. **83**, 555 (1979).

[14] D. F. Nelson, R. C. Miller, C. W. Tu, and S. K. Sputz, Phys. Rev. B **36**, 8063 (1987).

[15] J. Christen and D. Bimberg, Phys. Rev. B **42**, 7213 (1990); J. Christen, Festkörperprobleme **30**, 239 (1990).

[16] M. Zachau, J. A. Kash, and W. T. Masselink, Phys. Rev. B **44**, 8403 (1991).

[17] D. Gammon, B. V. Shanabrook, and D. S. Katzer, Phys. Rev. Lett. **67**, 1547 (1991).

[18] B. M. Ashkinadze, E. Cohen, Arza Ron, and L. N. Pfeiffer, Phys. Rev. B **47**, 10 613 (1993).

[19] T. Takagahara, Phys. Rev. B **31**, 6552 (1985). For the calculation we used the following parameters taken from this paper: $a_B=100$ Å, $m_e=0.067m_0$, $m_{\rm hh}=0.45m_0$, $u_{\rm LA}=4.81\times10^5$ cm/sec, $D_c=-6.5$ eV, $D_v=3.1$ eV.